Electronic Supplementary Material (ESI) for Chemical Communications.

Supporting Information

Structural snapshots of the SCR reaction mechanism on Cu-SSZ-13

Tobias Günter[†], Hudson W.P. Carvalho[†], Dmitry E. Doronkin[†,‡], Thomas Sheppard[†], Pieter Glatzel[§], Andrew J. Atkins[ζ], Julian Rudolph[ξ], Christoph R. Jacob[ζ,ξ], Maria Casapu[†], Jan-Dierk Grunwaldt[†,‡]*

[†]Institute for Chemical Technology and Polymer Chemistry, KIT, Kaiserstr. 12, D-76131 Karlsruhe, Germany

[‡] Institute of Catalysis Research and Technology, KIT, Hermann-von-Helmholtz-Platz 1, D-76344 Eggenstein-Leopoldshafen, Germany

[§] European Synchrotron Radiation Facility, 6 rue Jules Horowitz, BP 220, F-38043 Grenoble Cedex, France

[ζ] Center for Functional Nanostructures and Institute of Physical Chemistry, Karlsruhe Institute of Technology, Wolfgang-Gaede-Str. 1a, D-76131 Karlsruhe, Germany

[ξ] Institute of Physical and Theoretical Chemistry, TU Braunschweig, Hans-Sommer-Str. 10, D-38106 Braunschweig, Germany

S1. Catalyst preparation

Na-SSZ-13 was prepared by a method similar to Deka[1] and Zones[2]. First, 0.67 g sodium hydroxide, 41.1 g deionised water, 14.8 g N,N,N-trimethyladamantylammonium hydroxide (TMAdOH, 25 wt %, Sachem) and 0.43 g aluminium hydroxide were mixed for 30 min. 13.0 g colloidal silica (Ludox® AS-40) was added and stirred for another 10 min. The as prepared gel was transferred into a 200 ml Teflon-lined autoclave and aged at room temperature for 2 h. The gel was then heated statically for 4 days at 160 °C. The resulting suspension was filtered, washed with 1 L deionised water and dried at 80 °C before calcination at 550 °C for 2 h.

As prepared Na-SSZ-13 was ion exchanged with aqueous 1 M NH_4NO_3 solution (20 mL/g zeolite) for 2 h at 75 °C, washed with deionised water, dried at 80 °C and calcined at 550 °C for 2 h. These steps were repeated for further two times without calcination at the final step to receive NH_4-SSZ-13.

Cu was introduced via liquid ion exchange of 2 g NH_4-SSZ-13 in 200 ml 0.005 M $Cu(OAc)_2$ solution at room temperature for 24 h. The slurry was filtered, washed with 1 L deionised water, dried at 80 °C and calcined at 550 °C for 8 h.

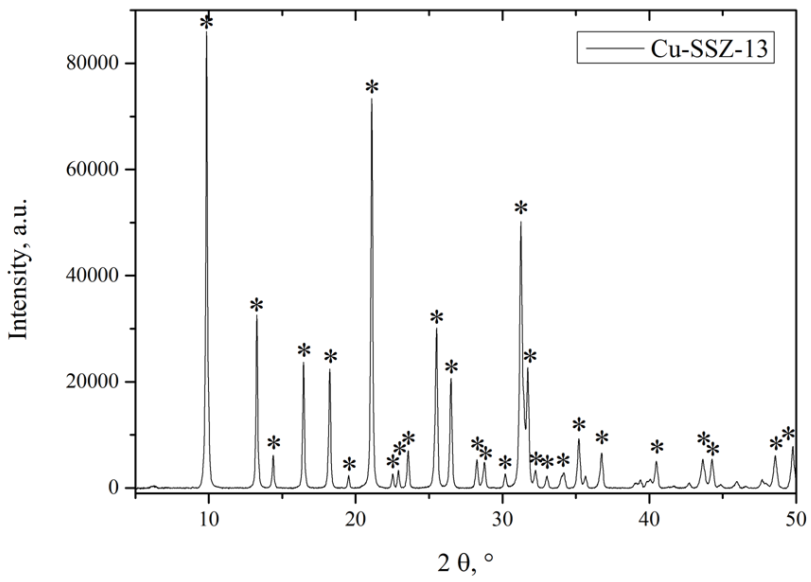

Figure S1. X-ray diffraction pattern of synthesized Cu-SSZ-13 (marked reflexes for SSZ-13 according to literature[2-3])

The X-ray diffraction pattern confirms the chabazite structure, no other crystalline impurities or proof for Cu_xO_y-moieties can be observed.

Elemental analysis by X-ray fluorescence (XRF) gave a Si/Al-ratio of 16 and a Cu/Al-ratio of 0.2. The BET-surface area is 590 m^2/g with a total pore volume of 0.33 cm^3/g.

S2. Experimental Details and further results on catalytic performance

Catalytic tests with the laboratory setup were performed under steady-state conditions in a fixed-bed plug flow reactor setup. 250 mg of powder sample (sieve fraction: 125 - 250 µm) was diluted with 250 mg quartz sand (same sieve fraction) and loaded in a tubular quartz reactor (inner diameter: 8 mm). Prior to the experiment, the catalyst was pre-treated at 550 °C in 10% O_2 in N_2 for 1 h. Afterwards, the desired reaction temperature was adjusted and the corresponding gas mixture was dosed: 1000 ppm NO, 1000 ppm NH_3, 0 - 1.5 % H_2O, 10 % O_2 and N_2 balance

with a total flow of 1.84 l/min corresponding to a Gas Hourly Space Velocity (GHSV) of 200 000 h^{-1}. Reaction products were monitored by an MKS MultiGas 2030 FTIR analyzer.

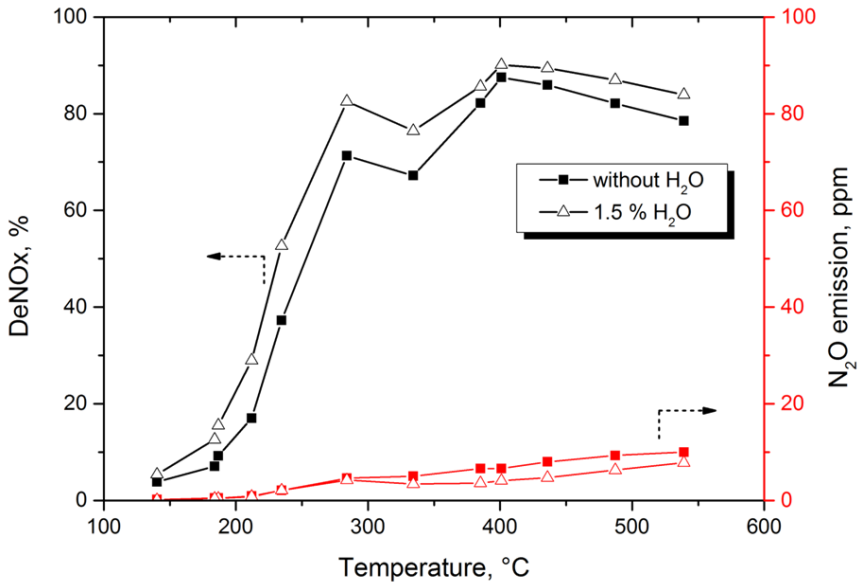

Figure S2. Catalytic activity of studied Cu-SSZ-13 measured in the laboratory. Conditions: 1000 ppm NO, 1000 ppm NH_3, 10% O_2, 0 - 1.5% H_2O, N_2 balance; GHSV = 200 000 h^{-1}.

The Cu-SSZ-13 catalyst shows a similar SCR activity as known from literature for such catalysts.[4] At this high space velocity, the seagull shape is observed as also reported by Gao et al.[5] for low Cu loadings. A positive influence of water can be observed for the entire temperature regime.

S3. EXAFS-measurements

Ex situ EXAFS measurements were performed at the XAS - beamline (equipped with a bending magnet and Si(111) monochromator) at ANKA (Karlsruhe, Germany). The spectra were recorded in transmission mode at Cu K edge (8979 eV). The data was normalized and the extended X-ray absorption fine structure spectra (EXAFS) were background subtracted using the AUTOBKG algorithm in Athena.[6] The k^3-weighted EXAFS functions ($k^3\chi(k)$) were Fourier

transformed in the k range of 3.0-11 $Å^{-1}$ and multiplied by a Hanning window with sills size of 1 $Å^{-1}$. The refinement was carried out using Arthemis code[6], a structural model based on the local chemical environment of CuO was set up using *.cif*-file from the ICSD database (collection code 16025). Then the corresponding theoretical backscattering amplitudes and phases were calculated by FEFF 6.0.[7] The theoretical data were adjusted to the experimental spectra by a least square method in R-space from 1.0-2.35 Å. The amplitude reduction factors (S_0^2) were calculated using a CuO reference compound. Then the coordination numbers (N), atomic distances (r), energy shift (ΔE_0) and mean square deviation of interatomic distances (σ^2) were refined. The absolute misfit between theory and experiment has been expressed by ρ.[8]

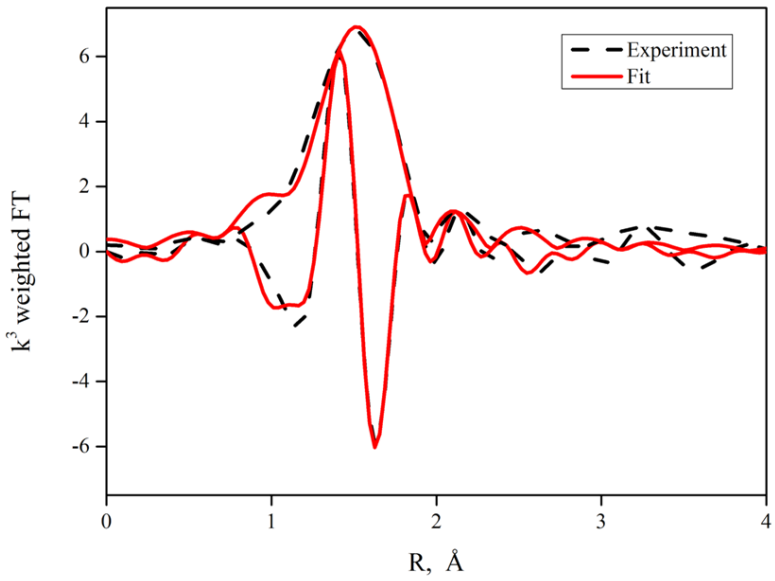

Figure S3. Fourier transformed k^3-weighted EXAFS spectra at the Cu K-edge for the as-prepared Cu-SSZ-13 catalyst. The Fit results showed 3.8 ± 0.3 O atoms around Cu, bond length of 1.96 ± 0.02 Å, ΔE_0 of -2.2 ± 1.1 eV, σ^2 of 0.0045 ±0.001 $Å^2$ and ρ of 0.7%. The absence of further shells suggests that Cu might be regarded as isolated 4-fold coordinated sites.

S4. HERFD-XANES and XES experiments

S4.1 Experimental

High-energy-resolution fluorescence-detected (HERFD) X-ray absorption near edge structure (XANES) and X-ray emission spectroscopy (XES) measurements were performed at the ID26 beamline of the European Synchrotron Radiation Facility (ESRF, Grenoble, France). The experimental setup employed in the present study is illustrated in Figure S4.

The catalyst (7 mg, sieved fraction 100-200 μm, 8 mm bed length) was placed in a 1 mm quartz capillary (20 μm walls) which served as a plug-flow reactor[9-10] heated by a hot gas blower (FMB Oxford). The gas composition was analyzed by an online Fourier Transform infrared spectroscopy (FTIR) (MKS 2030) analyzer. The catalyst response was followed at about 200 °C and 400 °C (under full SCR feed only) in a gas stream of 25 – 30 ml/min containing 0 – 1000 ppm NO, 0 – 1000 ppm NH_3, 10% O_2, 0 - ~1.5% H_2O in He (reactive mixtures), in 21% O_2 , 0 - ~1.5% H_2O in He (synthetic air), or in pure He. Note that in the laboratory setup usually nitrogen is used as inert gas. GHSV was kept at ~200 000 h^{-1}. Hence, the experiment was as close as possible to the laboratory setup (Figure 1). The X-ray beam size was 0.2 x 1 mm positioned at the beginning of the catalyst bed for the in situ / operando studies (additional positions along the catalyst bed were measured as well) and 0.2 x 0.7 mm for measurement of the reference samples in form of pellets.

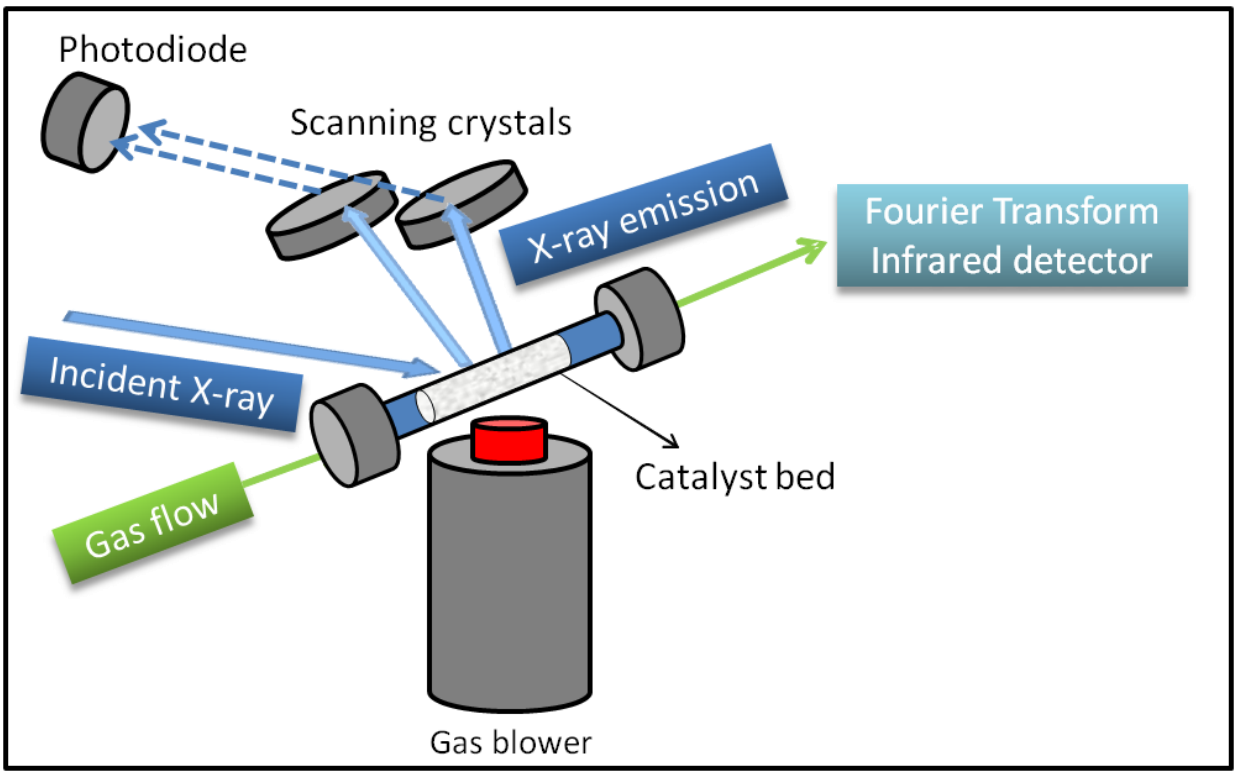

Figure S4. Mircroreactor setup based on a quartz capillary with gas blower at beamline ID26 at ESRF (Grenoble, France)

Synchrotron radiation at beamline ID26 is provided by three mechanically independent undulators. The higher harmonics were suppressed by Si coated mirrors which operate in total reflection mode. The desired energy was selected by a Si(111) double crystal monochromator and the beam was horizontally and vertically focalized by a pair of mirrors. The fluorescence X-rays were collected by an X-ray spectrometer using the (800) reflection of two spherically bent Ge crystals, the photons were counted by an avalanche photodiode. The monochromator energy calibration was performed by measuring Cu foil in transmission mode. The spectrometer energy calibration was carried out by keeping the spectrometer energy set at 8903 eV and scanning the energy of the monochromator to record the elastic peak.

For the HERFD-XANES measurements the monochromator energy was scanned while the spectrometer was kept fixed at the maximum of the $K\beta_{1,3}$ emission line (8903.6 eV). The spectra were normalized using the Athena software based on the edge step.

In turn, for the XES measurements the incident energy coming from the monochromator was kept constant at 9100.0 eV, *i.e*. above the Cu K absorption edge, and the spectrometer scanned the X-rays emitted by the sample. The valence-to-core spectra recorded in different conditions (temperature, gases) were first normalized based on the area of the $K\beta_{1,3}$ emission lines, this procedure aims at correcting for any changes in the intensity due to the heterogeneities on the sample. For the valence-to-core data on the tail of the $K\beta_{1,3}$ emission line the background was subtracted. For that, four pseudo Voigt functions were used, more details on this procedure can be found in [11].

S4.2 Results

Reference compounds with known structure (details in Table S1) were measured to interpret the influence of the coordination number and oxidation state on the XANES and XES spectra (Figure S5).

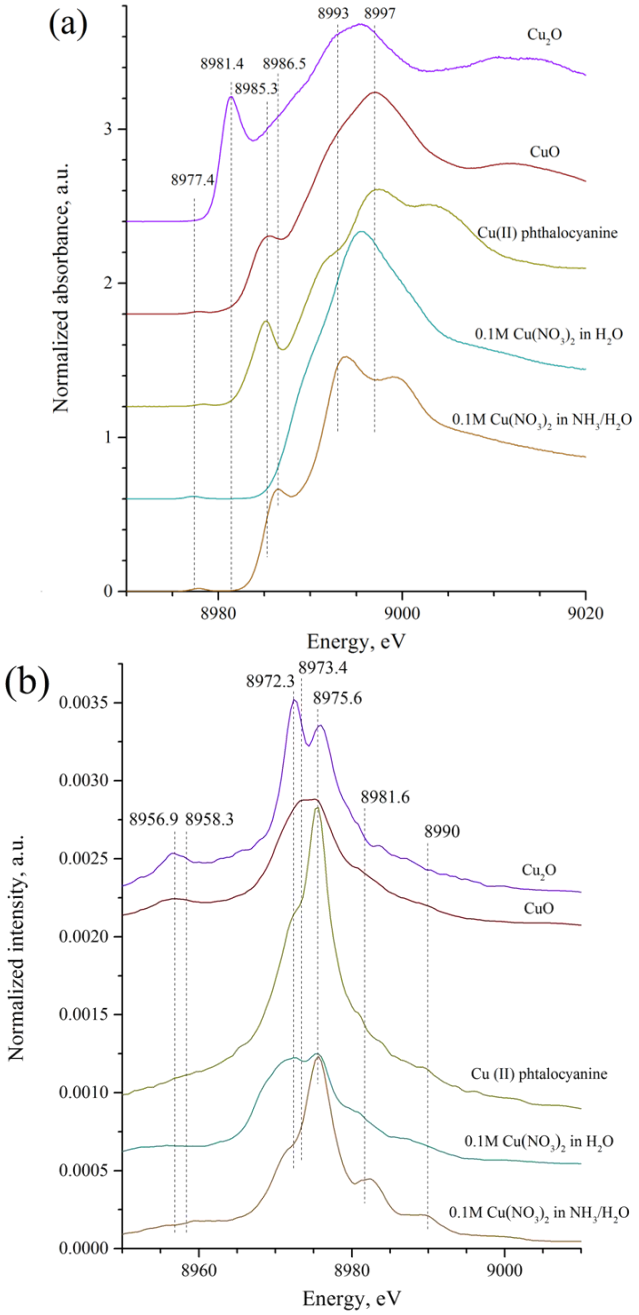

Figure S5. (a) HERFD-XANES and (b) XES spectra of reference structures.

The results obtained with HERFD-XANES in a gas mixture with/without NH_3 are plotted separately in an overlapping mode to obtain a clearer image of the differences induced by the variation of the gas composition (Table S2). Summary of the encountered differences of the HERFD-XANES and also of the XES is reported in Table S3.

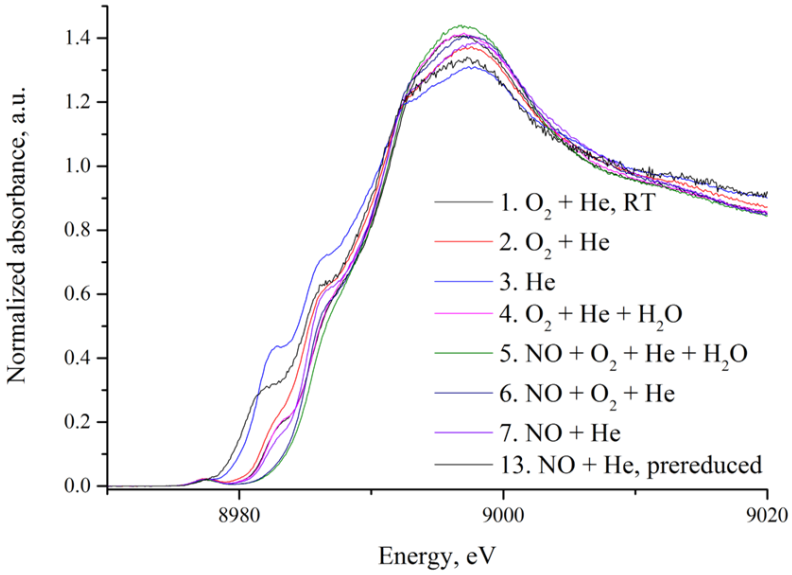

Figure S6. HERFD-XANES of Cu-SSZ-13 catalyst under gas feeds without NH_3

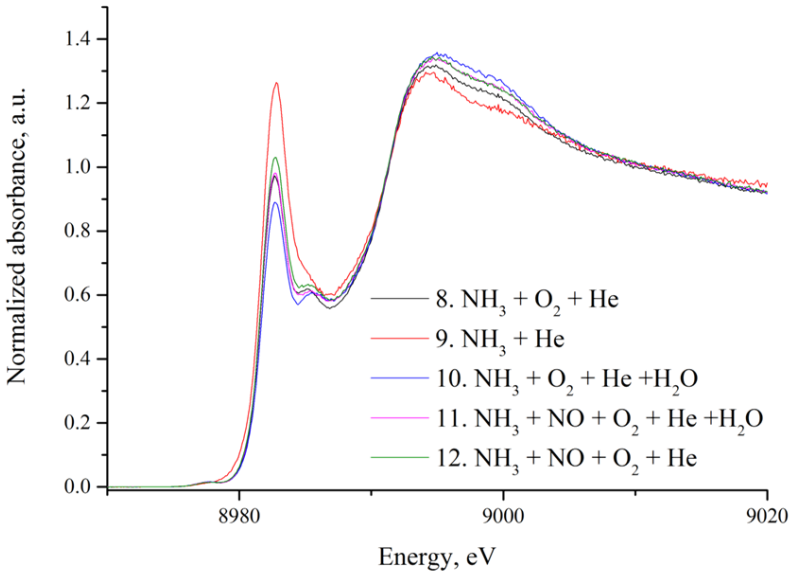

Figure S7. HERFD-XANES of Cu-SSZ-13 catalyst under gas feeds with NH_3

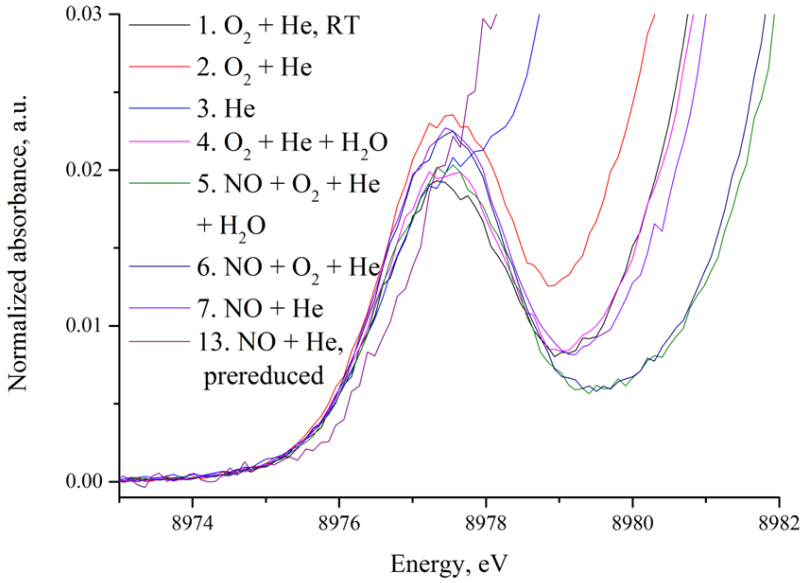

Figure S8. Pre-edge region of HERFD-XANES of Cu-SSZ-13 under gas feeds without NH_3

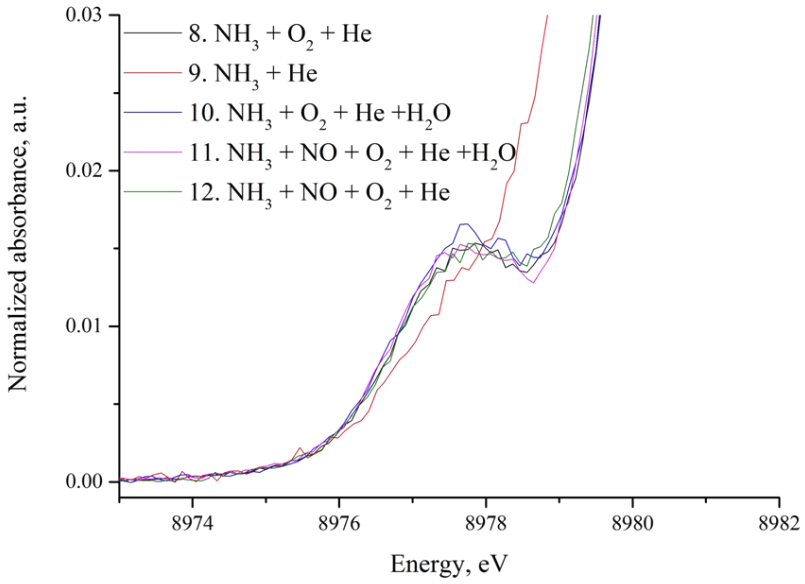

Figure S9. Pre-edge region of HERFD-XANES of Cu-SSZ-13 catalyst under gas feeds with NH_3

Table S1. Summary of the features of HERFD-XANES and XES spectra of reference substances (relative intensities of features semi-quantitatively given from - (not observed) to +++ (strongly pronounced)).

Reference substance	**XANES pre-edge and edge features / position (eV)**						**XES K β" / position (eV)**		**XES K $\beta_{2,5}$ / position (eV)**					**State of Cu**
	8977.4	8981.4	8985.3	8986.5	~8993	~8997	8956.9	8958.3	8972.3	8973.4	8975.6	8981.6	8990	
Cu_2O	-	+	-	-			+	-	++	-	+	-	-	Tetrahedral Cu^+
CuO	+ (shifted)	-	+	-		+	+	-	-	+	+	-/+	-/+	Octahedral Cu^{2+}
Cu (II) phthalocyanine	+ (8978.3)	-	+	-		+	-	-/+	+	-	+++	-	+/-	Square-planar Cu^{2+}
0.1M water solution of $Cu(NO_3)_2$	+	-	-	-/+			+/-	-	+	-	+	-/+	-	Octahedral Cu^{2+}
0.1M water / ammonia solution of $Cu(NO_3)_2$	+ (8977.8)	-	-	+	+	+	-	+	+	-	++	++	+	Octahedral Cu^{2+}

Table S2. Summary of the gas concentrations under model and reaction conditions

#	Conditions	Temperature	Gas concentrations				
			NH_3	NO	H_2O	O_2	He
1[a]	O_2 + He	20 ℃	-	-	-	21 %	balance
2[b]	O_2 + He	200 ℃	-	-	-	21 %	balance
3	He	200 ℃	-	-	-	-	100 %
4	O_2 + He + H_2O	200 ℃	-	-	1.5 %	10 %	balance
5	NO + O_2 + He + H_2O	200 ℃	-	1000 ppm	1.5 %	10 %	balance
6	NO + O_2 + He	200 ℃	-	1000 ppm	-	10 %	balance
7	NO + He	200 ℃	-	1000 ppm	-	-	balance
8	NH_3 + O_2 + He	200 ℃	1000 ppm	-	-	10 %	balance
9	NH_3 + He	200 ℃	1000 ppm	-	-	-	balance
10	NH_3 + O_2 + He + H_2O	200 ℃	1000 ppm	-	1.5 %	10 %	balance
11	NH_3 + NO + O_2 + He + H_2O	200 ℃	1000 ppm	1000 ppm	1.5 %	10 %	balance
12	NH_3 + NO + O_2 + He	200 ℃	1000 ppm	1000 ppm	-	10 %	balance
13[c]	NO + He	200 ℃	-	1000 ppm	-	-	balance

Table S3. Summary of the features of HERFD-XANES and XES spectra observed under different in situ and operando conditions. Quantification of approximate Cu^{2+} amount (±10%) relative to all Cu atoms in the sample made based on the intensity of the pre-edge peak (at 8977.4 eV) taking the intensity spectra measured under conditions 1,2,4-7 as Cu^{2+} reference (relative intensities of features semi-quantitatively given from - (not observed) to +++ (strongly pronounced)).

#	Conditions	XANES pre-edge and edge features / position (eV)						XES K β" / position (eV)		XES K $\beta_{2,5}$ / position (eV)					State of Cu (from the pre-edge)	Norm. abs. at 9002.5 eV
		8977.4	8982.7	8985.3	8986.5	~8993	~8997	8956.9	8958.3	8972.3	8973.4	8975.6	8981.6	8990		
1[a]	O_2 + He	+	+/-		-/+	+/-	+	+	-	+	-	++	+	+	90% Cu^{2+}	1.163
2[b]	O_2 + He	+	+/-		+/-	+/-	+	+	-	+	-	++	+	+	95% Cu^{2+}	1.157
3	He	+/-	+/-		+/-	+/-	+	+	-	+	-	++	+	+	40% Cu^{2+}	1.142
4	O_2 + He + H_2O	+	-, before XES +/-, after XES		-/+	-, before XES -/+, after XES	+	+	-	+	-	++	+	+	90% Cu^{2+}	1.177
5	NO + O_2 + He + H_2O	+	-		-/+	-/+	+	+	-	+	-	++	+	+	100% Cu^{2+}	1.177
6	NO + O_2 + He	+	-		-/+	+/-	+	+	-	+	-	++	+	+	100% Cu^{2+}	1.175
7	NO + He	+	-/+		+/-	+/-	+	+	?	+	-	++	+	+	100% Cu^{2+}	1.191
8	NH_3 + O_2 + He	-/+	+	+	-	+	+/-	?	+	-	+	+	++	++	50% Cu^{2+}	1.134
9	NH_3 + He	-/+	+	+/-	-	+	+/-	?	+	-	+	+	++	++	n.a.	1.133
10	NH_3 + O_2 + He + H_2O	+/-	+	+	-	+	+/-	?	+	-	+	+	++	++	45% Cu^{2+}	1.170
11	NH_3 + NO + O_2 + He + H_2O	+/-	+	+	-	+	+/-	?	+	-	+	+	++	++	45% Cu^{2+}	1.154
12	NH_3 + NO + O_2 + He	+	+	+	-	+	+/-	?	+	-	+	+	++	++	40% Cu^{2+}	1.157
13[c]	NO + He	-	+/-	-	+/-	+/-	+	+	-	+	-	++	+/-	+	n.a.	1.112

[a]XANES/XES performed at room temperature. [b]Pretreatment at 550 °C under the same gas mixture was performed. [c]Catalyst was reduced in 5% H_2/He at 550 °C prior to the measurement.

S5. DFT calculations

For the simulation of X-ray emission spectra, we considered three model structures in analogy to those employed in [12]. These structures were optimized with the ADF 2013.01 program package using unrestricted density-functional theory (DFT) with the BP86 exchange-correlation functional, a Slater-type TZP basis set, and an integration accuracy of 5. In this optimization, the structure of the zeolite framework was kept fixed. The optimized structures are shown in the upper part of Fig. S10. All model structures feature Cu in the formal oxidation state +II. The X-ray emission spectra were then calculated with the ORCA 3.0.2 program (unrestricted single point DFT calculations, BP86 exchange-correlation functional, def2-QZVPP basis set). For all anions, the COSMO solvation model with default parameters was applied. The calculated spectra were convoluted using a Gaussian line shape with a FWHM of 1.5 eV. The energy scale of the calculated XES spectra is shifted by 227 eV in order to align them with the experimental spectra.

The calculated spectra depicted in the lower part of Fig. S10 show a clear influence of the nature of the ligands in the Kβ" region. The substitution of an OH ligand by NH_2 results in a shift towards higher energies, whereas the coordination of NH_2 on an oxygen atom shows only very small effects. In the $K\beta_{2,5}$ region, the addition of NH_2 to the ligation intensifies the first peak and decreases the high energy peak. Although the used structure is based on a simplified model, the results show a clear trend that supports our experimental findings.

To verify that these small models are sufficient for assigning of the effect of different ligands on the XES spectra, we also performed calculations for a larger variant of model (1), which includes the six-membered ring structure of Cu-SSZ-13. Our model is based on the one used by Lamberti and coworkers in Ref. [13] and is shown in Fig. S11. It was obtained using the same

methodology as described above, but in analogy to Ref. [13], the Si and O atoms in the outer sphere (highlighted in Fig. S11) where fixed during the geometry optimization, and no solvation model was applied during the geometry optimization. The comparison of the calculated XES spectra in Fig. S10 of the minimal model (1) and the analogous larger model shows qualitatively identical spectra in the relevant region.

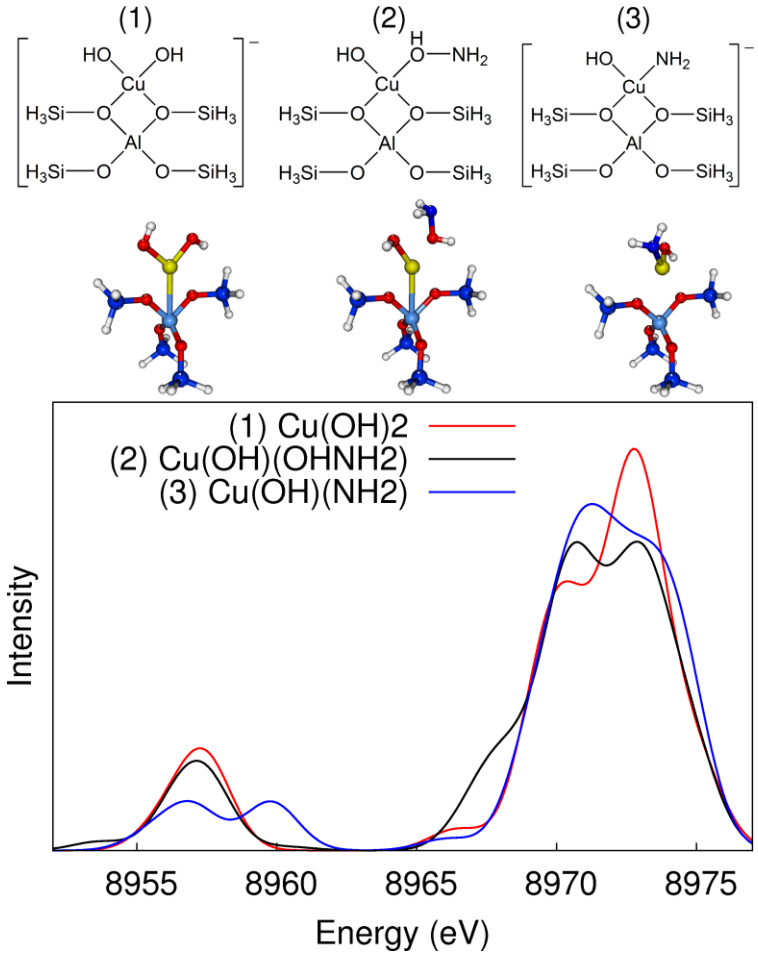

Figure S10. Calculated XES spectra of reference structures showing the effect of different ligand environment

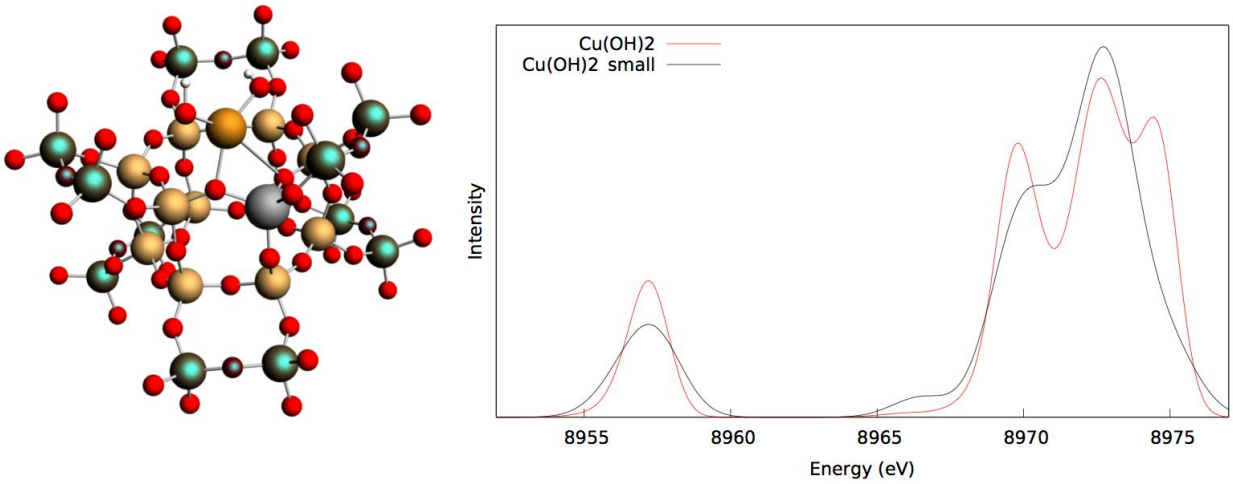

Figure S11. Left: Optimized structure of a larger variant of model (1) featuring two OH ligands at the Cu site (O: red, H: white, N: blue, Al: grey, Si: light brown, Cu: orange). The highlighted atoms (12 Si and 6 O) were frozen during the geometry optimization. Only the two hydrogen atoms of the two OH ligands are shown, all other hydrogen atoms hidden for clarity. Right: Calculated XES spectra of the minimal model (1) from Fig. S10 and for the larger model.

S6. Desorption experiments

Temperature Programmed Desorption (TPD) experiments for NH_3, NO and NO_2 have been performed to provide further details on the differences between Cu-SSZ-13 and Fe-ZSM-5 and the influence of water on the adsorption behavior.

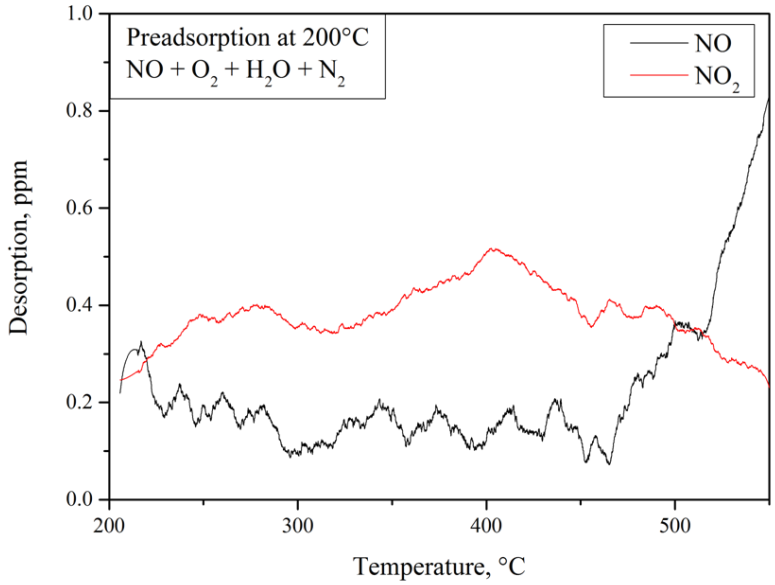

Figure S12. NO-TPD on Cu-SSZ-13 after saturation in 1000 ppm NO in the presence of 5 % H_2O and 10 % O_2 in N_2 at 200 °C.

The NO-TPD profile for Cu-SSZ-13 in Fig. S12 shows no desorption of NO or NO_2 after a saturation at 200°C in the presence of water and oxygen. This underlines the results observed by XANES and XES, where no NO-adsorption has been detected under these conditions.

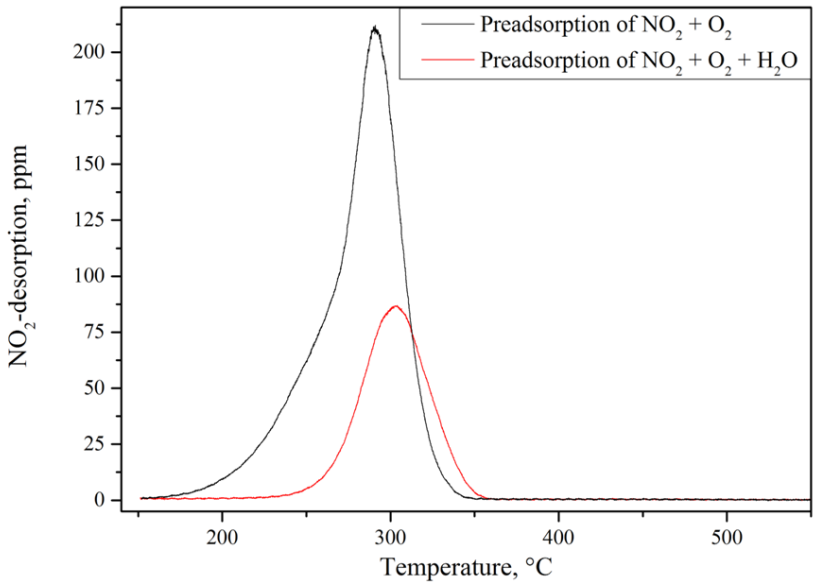

Figure S13. NO_2-TPD on Fe-ZSM-5 after saturation in 1000 ppm NO_2 with or without the presence of 5 % H_2O in 10 % O_2 and N_2 at 150 °C.

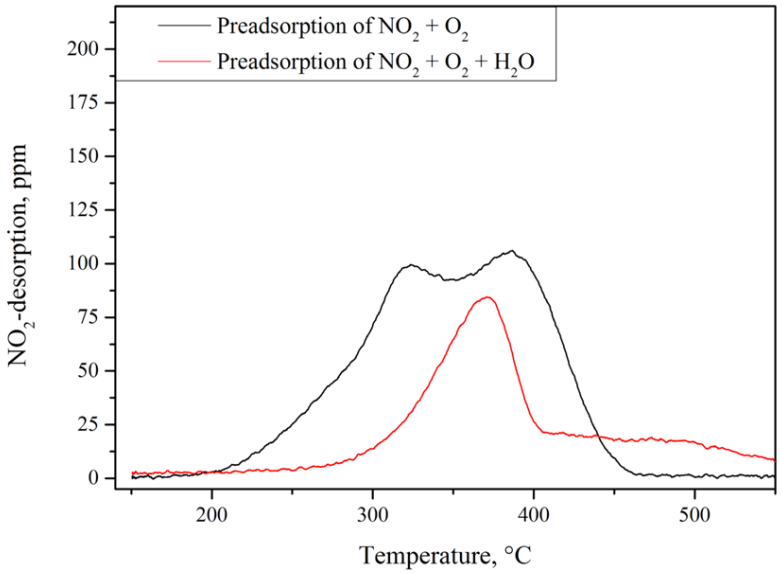

Figure S14. NO_2-TPD on Cu-SSZ-13 after saturation in 1000 ppm NO_2 with or without the presence of 5 % H_2O in 10 % O_2 and N_2 at 150 °C.

The NO_2-TPD results for Fe-ZSM-5 and Cu-SSZ-13 in Fig. S13 and S14 show a clear inhibition of the NO_2 adsorption by H_2O. Although NO_2 adsorbs on Cu-SSZ-13, no oxidation of NO to NO_2 has been observed at this temperature.

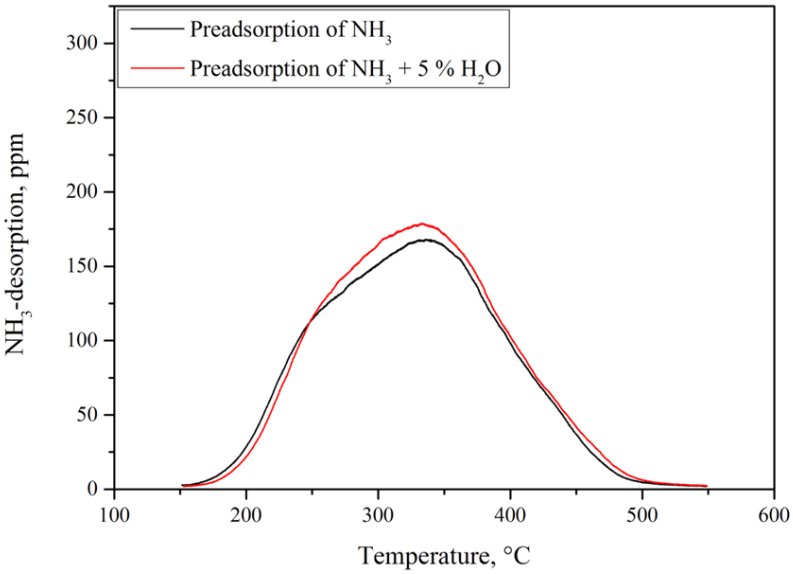

Figure S15. NH_3-TPD on Fe-ZSM-5 after saturation in 1000 ppm NH_3 with or without the presence of 5 % H_2O in N_2 at 150 °C.

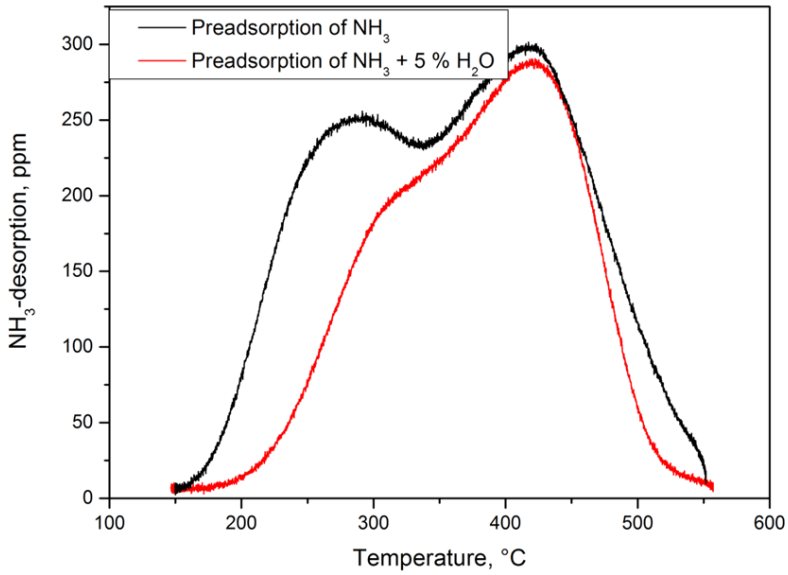

Figure S16. NH_3-TPD on Cu-SSZ-13 after saturation in 1000 ppm NH_3 with or without the presence of 5 % H_2O in N_2 at 150 °C.

The NH_3-TPD profile for Fe-ZSM-5 in Fig. S15 does not show any influence of H_2O on the adsorbed NH_3, therefore NH_3 seems to be stronger bound than H_2O, which is in line with the observed inhibiting effect by NH_3 on Fe-ZSM-5. In constrast, a clear influence on the NH_3-TPD profile is observed for Cu-SSZ-13 in Fig. S16. The low temperature peak is less pronounced, which confirms the competitive adsorption of NH_3 and H_2O.

References

1. Deka, U.; Lezcano-Gonzalez, I.; Warrender, S. J.; Lorena Picone, A.; Wright, P. A.; Weckhuysen, B. M.; Beale, A. M. Changing active sites in Cu–CHA catalysts: deNOx selectivity as a function of the preparation method. *Micropor. Mesopor. Mat.* **2013,** *166* (0), 144-152.
2. Zones, S. I. Zeolite SSZ-13 and its method of preparation. 4544538, 01.10.1985, 1985.
3. Kispersky, V. F.; Kropf, A. J.; Ribeiro, F. H.; Miller, J. T. Low absorption vitreous carbon reactors for operando XAS: a case study on Cu/Zeolites for selective catalytic reduction of NOx by NH_3. *Phys. Chem. Chem. Phys.* **2012,** *14* (7), 2229-2238.
4. Kwak, J.; Tran, D.; Szanyi, J.; Peden, C. F.; Lee, J. The Effect of Copper Loading on the Selective Catalytic Reduction of Nitric Oxide by Ammonia Over Cu-SSZ-13. *Catal. Lett.* **2012,** *142* (3), 295-301.
5. Gao, F.; Walter, E. D.; Kollar, M.; Wang, Y.; Szanyi, J.; Peden, C. H. F. Understanding ammonia selective catalytic reduction kinetics over Cu/SSZ-13 from motion of the Cu ions. *J. Catal.* **2014,** *319* (0), 1-14.
6. Ravel, B.; Newville, M. ATHENA, ARTEMIS, HEPHAESTUS: data analysis for X-ray absorption spectroscopy using IFEFFIT. *J. Synchrotron Radiat.* **2005,** *12* (4), 537-541.
7. Rehr, J.; Albers, R. Theoretical approaches to x-ray absorption fine structure. *Rev. Mod. Phys.* **2000,** *72* (3), 621-654.
8. Calvin, S.; Carpenter, E. E.; Ravel, B.; Harris, V. G.; Morrison, S. A. Multiedge refinement of extended x-ray-absorption fine structure of manganese zinc ferrite nanoparticles. *Phys. Rev. B* **2002,** *66* (22), 224405.
9. Clausen, B.; Gråbæk, L.; Steffensen, G.; Hansen, P.; Topsøe, H. A combined QEXAFS/XRD method for on-line, in situ studies of catalysts: Examples of dynamic measurements of Cu-based methanol catalysts. *Catal. Lett.* **1993,** *20* (1-2), 23-36.
10. Grunwaldt, J. D.; Caravati, M.; Hannemann, S.; Baiker, A. X-ray absorption spectroscopy under reaction conditions: suitability of different reaction cells for combined catalyst characterization and time-resolved studies. *Phys. Chem. Chem. Phys.* **2004,** *6* (11), 3037-3047.
11. Gallo, E.; Glatzel, P. Valence to Core X-ray Emission Spectroscopy. *Adv. Mater.* **2014,** *26* (46), 7730-7746.
12. Boubnov, A.; Carvalho, H. W. P.; Doronkin, D. E.; Günter, T.; Gallo, E.; Atkins, A. J.; Jacob, C. R.; Grunwaldt, J.-D. Selective Catalytic Reduction of NO Over Fe-ZSM-5: Mechanistic Insights by Operando HERFD-XANES and Valence-to-Core X-ray Emission Spectroscopy. *J. Am. Chem. Soc.* **2014,** *136* (37), 13006-13015.
13. Giordanino, F.; Borfecchia, E.; Lomachenko, K. A.; Lazzarini, A.; Agostini, G.; Gallo, E.; Soldatov, A. V.; Beato, P.; Bordiga, S.; Lamberti, C. Interaction of NH_3 with Cu-SSZ-13 Catalyst: A Complementary FTIR, XANES, and XES Study. *J. Phys. Chem. Lett.* **2014,** *5* (9), 1552-1559.